THE JOURNAL OF BIOLOGICAL CHEMISTRY VOL. 289, NO. 3, pp. 1519–1528, January 17, 2014

Mitochondria Contribute to NADPH Generation in Mouse Rod Photoreceptors*

Received for publication, August 16, 2013, and in revised form, November 25, 2013 Published, JBC Papers in Press, December 2, 2013, DOI 10.1074/jbc.M113.511295

Leopold Adler IV[‡], **Chunhe Chen**[‡], **and Yiannis Koutalos**[‡§1]

From the Departments of [‡]*Ophthalmology and* [§]*Neurosciences, Medical University of South Carolina, Charleston, South Carolina 29425*

Background: The major source of NADPH is considered to be the pentose phosphate pathway.
Results: In isolated mouse rod photoreceptors, blocking metabolite entry into mitochondria substantially reduces NADPH generation. Mitochondrial metabolic substrates support NADPH generation.
Conclusion: Mitochondria-linked pathways contribute substantially to NADPH generation in mouse rod photoreceptors.
Significance: A wide range of photoreceptor cell functions depend on adequate NADPH supply.

NADPH is the primary source of reducing equivalents in the cytosol. Its major source is considered to be the pentose phosphate pathway, but cytosolic $NADP^+$-dependent dehydrogenases using intermediates of mitochondrial pathways for substrates have been known to contribute. Photoreceptors, a nonproliferating cell type, provide a unique model for measuring the functional utilization of NADPH at the single cell level. In these cells, NADPH availability can be monitored from the reduction of the all-*trans*-retinal generated by light to all-*trans*-retinol using single cell fluorescence imaging. We have used mouse rod photoreceptors to investigate the generation of NADPH by different metabolic pathways. In the absence of extracellular metabolic substrates, NADPH generation was severely compromised. Extracellular glutamine supported NADPH generation to levels comparable to those of glucose, but pyruvate and lactate were relatively ineffective. At low extracellular substrate concentrations, partial inhibition of ATP synthesis lowered, whereas suppression of ATP consumption augmented NADPH availability. Blocking pyruvate transport into mitochondria decreased NADPH availability, and addition of glutamine restored it. Our findings demonstrate that in a nonproliferating cell type, mitochondria-linked pathways can generate substantial amounts of NADPH and do so even when the pentose phosphate pathway is operational. Competing demands for ATP and NADPH at low metabolic substrate concentrations indicate a vulnerability to nutrient shortages. By supporting substantial NADPH generation, mitochondria provide alternative metabolic pathways that may support cell function and maintain viability under transient nutrient shortages. Such pathways may play an important role in protecting against retinal degeneration.

NADPH is a necessary cofactor for lipid and nucleotide biosynthesis and for many other cellular processes including maintenance of the cellular antioxidant system, nitric oxide synthesis, or the respiratory burst of immune cells (1). The oxidative phase of the pentose phosphate pathway, a branch of glycolysis, has long been considered the main pathway for the generation of cytosolic NADPH (see Fig. 1) (1, 2). NADPH can also be generated by cytosolic $NADP^+$-dependent dehydrogenases utilizing isocitrate and malate as substrates. These substrates originate from the mitochondria where they also participate in the TCA cycle (see Fig. 1) (3, 4). Proliferating cells have been known to utilize both the pentose phosphate and mitochondria-linked pathways to generate the substantial levels of NADPH necessary for anabolic reactions (5). In a living nonproliferating cell, it is not clear how much the different pathways contribute to NADPH generation or to what extent a cell can meet its NADPH requirements in the absence of glucose, using only substrates of mitochondrial metabolism such as glutamine.

Isolated vertebrate photoreceptors provide a unique system to address these questions in a nonproliferating cell type: the generation of NADPH can be monitored at the single cell level through its utilization in a reduction reaction. Thus, we have examined the generation of NADPH by different metabolic pathways in single living rod photoreceptor cells isolated from wild type mouse retinas. The outer segment compartment of a vertebrate rod photoreceptor is a specialized organelle responsible for the detection of light (6). A single mouse rod outer segment contains ~50 million molecules of the visual pigment rhodopsin, the primary light detector, packed at a concentration of ~3 mM (7). Rhodopsin contains 11-*cis*-retinal as chromophore for the detection of light. Light absorption isomerizes the 11-*cis*-chromophore to all-*trans*, generating an enzymatically active intermediate that leads to the conversion of light to an electrical signal. Photoactivated rhodopsin subsequently releases its chromophore in the form of all-*trans*-retinal, which is reduced to all-*trans*-retinol in a reaction that requires NADPH (8). In the presence of bright light, large quantities of all-*trans*-retinal are released, requiring an equivalent amount of NADPH for their reduction. Thus, the conversion of all-*trans*-

* This work was supported, in whole or in part, by National Institutes of Health Grant R01-EY014850. This work was also supported by an unrestricted grant to the Department of Ophthalmology at Medical University of South Carolina from Research to Prevent Blindness (New York). This work was conducted in a facility constructed with support from National Institutes of Health Grant C06 RR015455 from the Extramural Research Facilities Program of the National Center for Research Resources.
[1] To whom correspondence should be addressed: Dept. of Ophthalmology, Medical University of South Carolina, 167 Ashley Ave., Charleston, SC 29425. Tel.: 843-792-9180; Fax: 843-792-1723; E-mail: koutalo@musc.edu.

retinal to retinol[2] provides a measure of the availability of NADPH. Fig. 1 shows a diagram of the metabolic pathways that can generate NADPH linked to its utilization for the reduction of all-*trans*-retinal to retinol. The metabolic machinery of the rod photoreceptor is present in the inner segment of the cell, whereas the reduction of retinal to retinol takes place in the outer segment.

All-*trans*-retinal and retinol both fluoresce and have a large difference in excitation maxima (9), which allows for the differentiation of their fluorescence signals (10, 11). A ratio of the fluorescence excited by two appropriately chosen wavelengths (340 and 380 nm) reflects the all-*trans*-retinol to retinal ratio, which is a measure of the conversion of all-*trans*-retinal to retinol, and thereby of NADPH availability as well. Using fluorescence imaging of single living mouse rod photoreceptors, we have found that mitochondria-linked pathways can and do support the generation of substantial amounts of NADPH to sustain ongoing cellular functions. These findings demonstrate the importance of mitochondrial support and of metabolites other than glucose in the generation of NADPH in nonproliferating cells.

EXPERIMENTAL PROCEDURES

Animals—Wild type (129/Sv) and *Rpe65*$^{-/-}$ mice were from established colonies at the Medical University of South Carolina. The wild type colony was established from breeding pairs obtained from Harlan Laboratories (Indianapolis, IN); breeding pairs for the *Rpe65*$^{-/-}$ colony were a generous gift of Dr. T. M. Redmond. Animals were 2–3 months old and were kept in cyclic light with a 12-h light cycle (06:00–18:00). All animal procedures were carried out in accordance with protocols approved by the Institutional Animal Care and Use Committees of the Medical University of South Carolina and with the recommendations of the Panel on Euthanasia of the American Veterinary Medical Association. For experiments, the animals were dark-adapted overnight and sacrificed under dim red light, and the retinas were excised under either dim red or infrared light in mammalian physiological solution (130 mM NaCl, 5 mM KCl, 0.5 mM $MgCl_2$, 2 mM $CaCl_2$, 25 mM hemisodium-HEPES, 5 mM glucose, pH 7.40). Isolated rod photoreceptor cells were obtained as described (12). All experiments were carried out with metabolically intact rod photoreceptors (10), unless explicitly stated otherwise.

Solutions—All reagents were of analytical grade. Stock solution of oligomycin was prepared in Me_2SO and all-*trans*-retinol and -retinal in ethanol. For experiments, retinoids were added to a Ringer's solution containing 1% BSA as carrier. The final concentrations of Me_2SO or ethanol were at most 0.05 and 0.1%, respectively, and had no effect on the fluorescence measurements. Ouabain, 2-deoxy-glucose, and α-cyano-4-hydroxy-cinnamate (4-CIN)[3] were dissolved directly into physiological solution. Solutions did not contain bicarbonate (see "Discussion"), the reason being that for experiments with single isolated cells, we find that pH is better controlled with a HEPES buffer system.

Fluorescence Imaging—Fluorescence measurements were carried out as described previously (11, 12), on the stage of an inverted Zeiss Axiovert 100 microscope with a 40× oil immersion objective lens (N.A. = 1.3). Fluorescence was excited with narrow band pass (10-nm bandwidth) filters centered at 340 and 380 nm, and emission was collected for >420 nm. For an experiment, fluorescence images were initially recorded for the dark-adapted cell; the cell was subsequently bleached with >530-nm light for 1 min (12), and fluorescence images were recorded at different times after bleaching. For analysis, regions of interest were defined for the rod outer segment and for a background area; then the rod outer segment fluorescence was corrected for background. After background correction, the rod outer segment fluorescence intensities caused by retinal and retinol were obtained for each time point by subtracting the initial fluorescence intensities recorded for the dark-adapted cell. Subsequently, the ratio Fex-340/Fex-380 of the fluorescence intensities excited by 340- and 380-nm light was calculated for each time point after bleaching. Image acquisition and analysis were carried out using Slidebook (Intelligent Imaging Innovations, Denver, CO).

To measure the Fex-340/Fex-380 fluorescence ratios for all-*trans*-retinol and all-*trans*-retinal, broken off rod outer segments (rod outer segments separated from the rest of the cell) were loaded with 50 μM of either retinoid for 5 min, using 1% BSA as lipophilic carrier (10, 11). To determine the intracellular pH of rod outer segments, BCECF, a ratiometric pH-sensitive dye was used, following published procedures used with isolated salamander rod photoreceptors (13). Isolated mouse rod photoreceptors were incubated with 10 μM BCECF-AM for 30 min, followed by washes with Ringer's to remove remaining extracellular dye. BCECF fluorescence was excited with 495- and 440-nm light, and emission was measured >515 nm. The ratio F_{495}/F_{440} of the fluorescence intensities excited by 495 nm (F_{495}) and 440 nm (F_{440}) depends on pH. The F_{495}/F_{440} fluorescence ratio was converted to pH using a calibration curve obtained with BCECF (1 mM) in solutions of phosphate-buffered physiological saline with different pH.

The possible interference of 4-CIN fluorescence with the measurement of the Fex-340/Fex-380 ratio was assessed in control experiments with *Rpe65*$^{-/-}$ rods, which contain negligible amounts of retinoids (14). This allowed the measurement of the levels of 4-CIN fluorescence in the absence of any retinoid fluorescence, and we concluded that 4-CIN fluorescence did not interfere with the Fex-340/Fex-380 measurements (see Fig. 9).

Statistical Analysis—Statistical significance was tested with analysis of variance. In the figures, statistically significant differences are indicated with *asterisks*.

RESULTS

Measurement of NADPH from Fluorescence Ratios—Following light exposure of dark-adapted rod photoreceptors, all-*trans*-retinal is released from photoactivated rhodopsin and is converted to all-*trans*-retinol using NADPH as a cofactor

[2] When the isomer is not specified, retinal and retinol refer to the all-*trans* isomers.

[3] The abbreviations used are: 4-CIN, α-cyano-4-hydroxy-cinnamate; QYR, ratio of fluorescence quantum yield of retinol over that of retinal; RAL, all-*trans*-retinal; ROL, all-*trans*-retinol; BCECF, 2′,7′-bis(2-carboxyethyl)-5(6)-carboxyfluorescein.

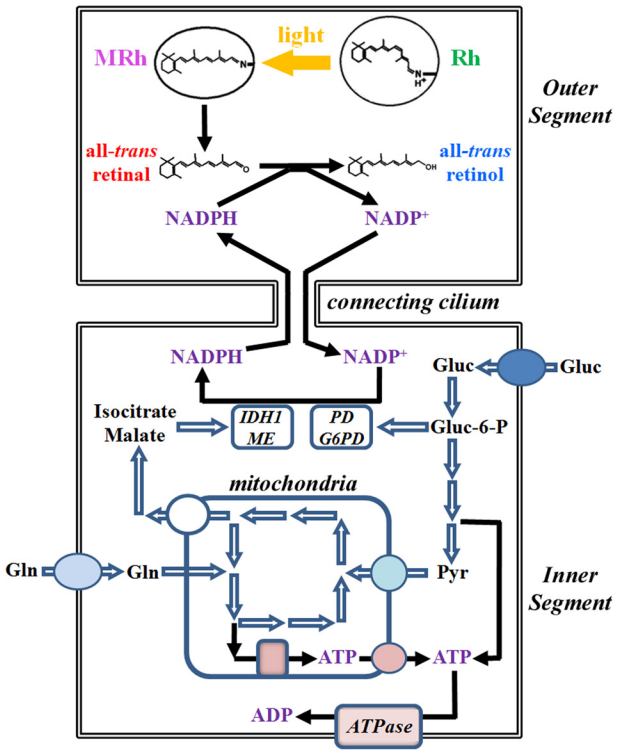

FIGURE 1. **Scheme for the generation of NADPH by rod inner segment metabolic pathways utilizing glucose and glutamine as substrates.** The generated NADPH is a necessary cofactor for the reduction of retinal to retinol in the rod outer segment. The metabolic substrate for the pentose phosphate pathway is glucose, which can enter the pathway after its phosphorylation to glucose-6-phosphate (*Gluc-6-P*) by a hexokinase. Through the pentose phosphate pathway, one molecule of glucose generates two molecules of NADPH: one is generated through the oxidation of glucose-6-phosphate to 6-phosphogluconolactone by glucose-6-phosphate dehydrogenase (*G6PD*), and one more is generated through the oxidative decarboxylation of 6-phosphogluconate to ribulose-5-phosphate by 6-phosphogluconate dehydrogenase (*PD*). NADPH can also be generated by cytosolic $NADP^+$-dependent isocitrate dehydrogenase 1 (*IDH1*) and malic enzyme (*ME*), which catalyze the oxidative decarboxylation of isocitrate to α-ketoglutarate and the oxidation of malate to pyruvate, respectively. Isocitrate and malate originate from the mitochondria where they also participate in the TCA cycle. *Rh*, rhodopsin; *MRh*, metarhodopsin; *Gluc*, glucose; *Gln*, glutamine; *Pyr*, pyruvate.

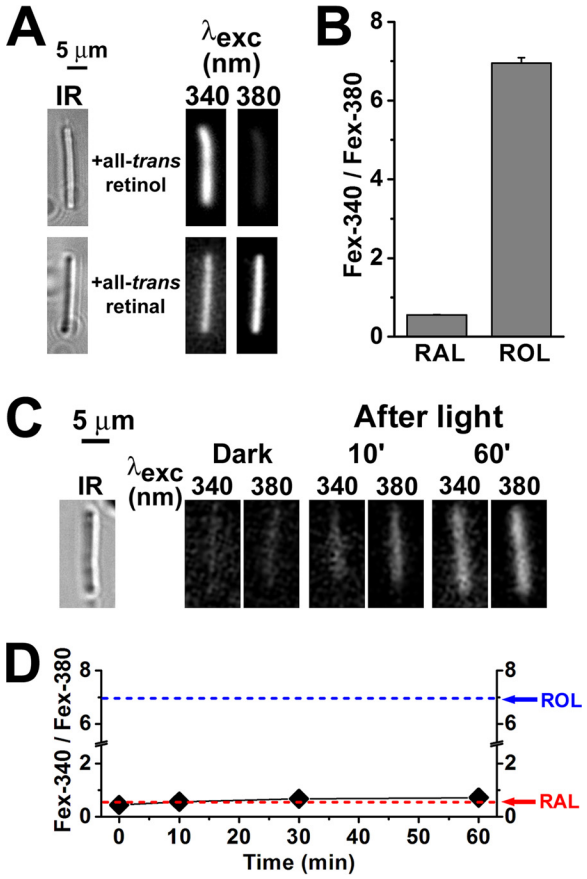

FIGURE 2. **Measurement of RAL and ROL Fex-340/Fex-380 fluorescence ratios.** Fluorescence was excited with 340- and 380-nm light, and emission was collected for >420 nm. *A*, fluorescence of mouse broken off rod outer segments (rod outer segments separated from the rest of the cell) loaded with 50 μM all-*trans*-retinol or all-*trans*-retinal (for 5 min, using 1% BSA as carrier). *IR*, infrared images of the outer segments. Fluorescence images of the outer segments after loading with retinoid are shown with the same intensity scaling to facilitate comparisons. *B*, values of the Fex-340/Fex-380 fluorescence intensity ratio for retinal and retinol, obtained by loading broken off rod outer segments with 50 μM RAL ($n = 6$ cells) and 50 μM ROL ($n = 8$ cells). *C*, mouse broken off rod outer segments cannot support the reduction of all-*trans*-retinal to retinol. *IR*, infrared image of an outer segment; fluorescence images of the outer segment before (*Dark*) and at different times after bleaching are shown with the same intensity scaling to facilitate comparisons; glucose concentration was 5 mM. *D*, dependence of the Fex-340/Fex-380 fluorescence intensity ratio on time after bleaching in broken off rod outer segments (◆, $n = 6$), in the absence of any exogenously added retinoid. The *arrows* point to the values of the ratio for RAL and ROL as determined in *B*. The value of the fluorescence ratio for the endogenous retinoid that appears after bleaching is similar to that for all-*trans*-retinal. All experiments were performed at 37 °C.

(Fig. 1). As retinal and retinol fluoresce with excitation maxima at different wavelengths, this conversion can be monitored from the relative intensities of the rod outer segment fluorescence excited by 340 and 380 nm. The ratio Fex-340/Fex-380 of the intensities of the fluorescence excited by 340- and 380-nm light is a measure of the fraction of the released all-*trans*-retinal converted to all-*trans*-retinol (10, 11). The conversion depends on the availability of NADPH. In the absence of any available NADPH, there would be no conversion, and the fluorescence would be due solely to all-*trans*-retinal. On the other hand, if most of the NADP were maintained in the reduced form, the released retinal would be fully converted, and the fluorescence would be due solely to retinol. The values of the Fex-340/Fex-380 ratio for retinal and retinol were obtained by loading broken off rod outer segments with 50 μM of each retinoid. The values of the ratios were 0.55 ± 0.01 ($n = 6$) for retinal and 6.95 ± 0.14 ($n = 8$) for retinol (Fig. 2, *A* and *B*). These values correspond to limits of 0 and 1 for the fraction of NADPH present and are in close agreement with the values determined and reported previously for the inverse ratio Fex-380/Fex-340 (11). Broken off rod outer segments were used for these control measurements because they are separated from the metabolic machinery of the cell and cannot process retinal or retinol (10, 11). Thus, in a broken off rod outer segment, the all-*trans*-retinal released from photoactivated rhodopsin has no access to NADPH and is not converted to all-*trans*-retinol to any significant degree (Fig. 2, *C* and *D*).

The Fex-340/Fex-380 ratio was chosen because it increases with the proportion of released retinal converted to retinol and with the fraction of NADP present in the reduced form of NADPH. Assuming that the reduction reaction in Equation 1 is close to equilibrium, a relationship between the Fex-340/Fex-380 ratio and the fraction of NADPH can be obtained.

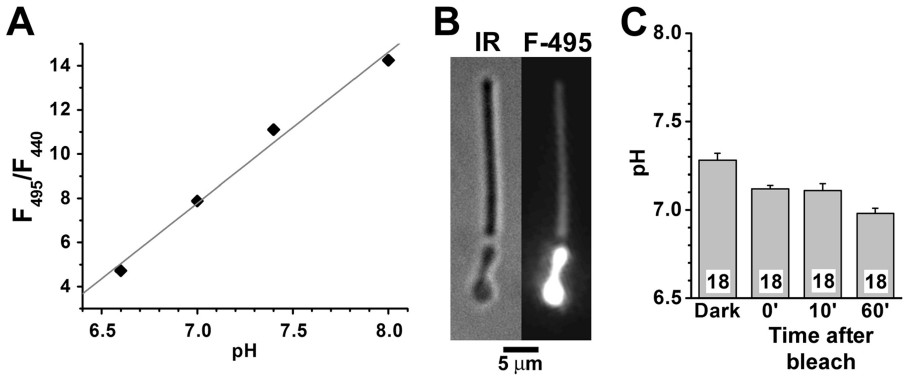

FIGURE 3. **Determination of outer segment pH in isolated mouse rod photoreceptors with BCECF, a ratiometric pH-sensitive dye.** BCECF fluorescence was excited with 495- and 440-nm light, and emission was measured >515 nm. *A*, calibration curve for BCECF (1 mM) in phosphate-buffered physiological saline; three determinations at each pH. The standard error bars that do not appear in the graph were smaller than symbol size. The *straight line* is a least squares fit to the data points, giving pH = 5.86 + 0.15 × F_{495}/F_{440}. This equation was used to convert the F_{495}/F_{440} fluorescence ratio to pH. *B*, infrared (*IR*) bright field and fluorescence (495-nm excitation) images of an isolated mouse rod photoreceptor loaded with BCECF. *C*, outer segment pH of isolated mouse rod photoreceptors before (*Dark*) and at different times after bleaching. The numbers of cells are shown within each column; the cells for *Dark* and at 0 and 10 min after bleaching were the same (a cell was selected, bleached and fluorescence was measured until 10 min after bleaching); different cells were used for the measurement 60 min after bleaching. All experiments, including calibrations, were performed at 37 °C.

$$\text{retinal} + \text{NADPH} + \text{H}^+ \leftrightarrow \text{retinol} + \text{NADP}^+ \quad \text{(Eq. 1)}$$

If ROL and RAL stand for all-*trans*-retinol and all-*trans*-retinal, respectively, and K_{eq} the equilibrium constant, then

$$K_{eq} = ([\text{RAL}] \times [\text{NADPH}] \times [\text{H}^+])/([\text{ROL}] \times [\text{NADP}^+]) \quad \text{(Eq. 2)}$$

If $r = [\text{ROL}]/([\text{RAL}] + [\text{ROL}])$ is the fraction of retinol, and the fraction of reduced NADP is $N_{red} = [\text{NADPH}]/([\text{NADPH}] + [\text{NADP}^+])$ by rearranging Equation 2, we obtain

$$N_{red} = r/([\text{H}^+]/K_{eq} + (1 - [\text{H}^+]/K_{eq}) \times r) \quad \text{(Eq. 3)}$$

The relationship between the fraction r of retinol and the ratio Fex-380/Fex-340 (the inverse of the ratio used here) has been derived before (Equation 4b in Ref. 11). If QYR is the ratio of fluorescence quantum yields for retinol and retinal (Equation 4a in Ref. 11) and

$$FR = \text{Fex-340/Fex-380} \quad \text{(Eq. 4)}$$

then

$$r = (1.8 \times \text{FR} - 1)/((1.8 \times \text{FR} - 1) + \text{QYR} \times (1 - 0.14 \times \text{FR})) \quad \text{(Eq. 5)}$$

After substituting Equation 5 into Equation 3, we obtain

$$N_{red} = (1.8 \times \text{FR} - 1)/((1.8 \times \text{FR} - 1) + ([\text{H}^+]/K_{eq}) \times \text{QYR} \times (1 - 0.14 \times \text{FR})) \quad \text{(Eq. 6)}$$

The values (1.8 = 1/0.55 and 0.14 = 1/6.95) of the parameters in Equation 5 were determined by loading broken off rod outer segments with 50 μM retinal or retinol (Fig. 2, *A* and *B*). Intracellular rod outer segment pH was measured with the fluorescent dye BCECF (13) (Fig. 3). The pH was ~7.3 before bleaching and decreased to 7.0–7.1 following bleaching, the reduction likely reflecting the generation of H^+ from light-stimulated cGMP hydrolysis. For calculations with Equation 6, a rod outer segment pH value of 7.0 was used. $K_{eq} = 3.3 \times 10^{-9}$ M

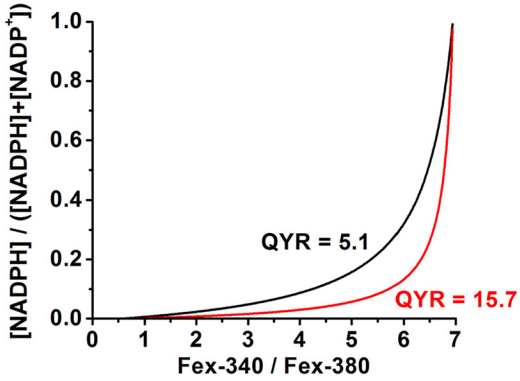

FIGURE 4. **Dependence of the fraction N_{red} = [NADPH]/([NADPH] + [NADP$^+$]) on the fluorescence ratio Fex-340/Fex-380.** The dependence has been calculated from Equation 6 for the two different values, 5.1 and 15.7, of the ratio QYR of the quantum yield of retinol over that of retinal. Fex-340 and Fex-380 are the fluorescence intensities excited by 340- and 380-nm light, respectively (emission, >420 nm).

(15). QYR has been determined before with two different approaches, and values of 5.1 and 15.7 have been obtained (11). The relation between N_{red}, the fraction of total NADP that is in the reduced form, and the ratio FR = Fex-340/Fex-380 is plotted in Fig. 4 for the two values of QYR and for rod outer segment, pH 7.0. In the rest of the paper and for simplicity of presentation, the value QYR = 5.1 is used to calculate the NADPH fractions corresponding to different values of the Fex-340/Fex-380 fluorescence ratio. The values of the NADPH fraction obtained using QYR = 15.7 are lower (Fig. 4).

Substrates of Mitochondrial Metabolism Support the Generation of NADPH—In the presence of 5 mM glucose, a large proportion of the released retinal is converted to retinol, as indicated by the much higher intensity of the fluorescence excited by 340 nm compared with that excited by 380 nm (Fig. 5). When glucose is used as a metabolic substrate, potential NADPH sources are the glucose-6-phosphate and 6-phosphogluconate dehydrogenases of the pentose phosphate pathway and cytosolic $NADP^+$-dependent dehydrogenases that utilize as substrates metabolites provided by the mitochondria (Fig. 1). In the absence of metabolic substrate, the similar intensities of the

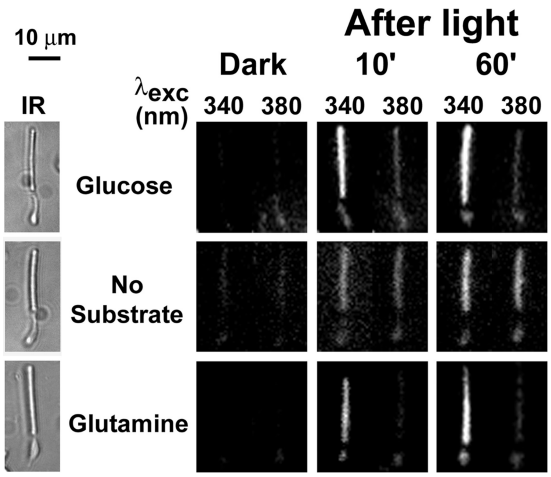

FIGURE 5. **Glutamine can support retinol formation in isolated mouse rod photoreceptors.** Retinol and retinal were distinguished by exciting fluorescence with 340- and 380-nm light and collecting emission for >420 nm. *IR*, infrared images of the cells; fluorescence images of the cells before (*Dark*) and at different times after bleaching are shown with the same intensity scaling to facilitate comparisons. Glucose concentration was 5 mM; glutamine concentration was 0.2 mM. Experiments were performed at 37 °C.

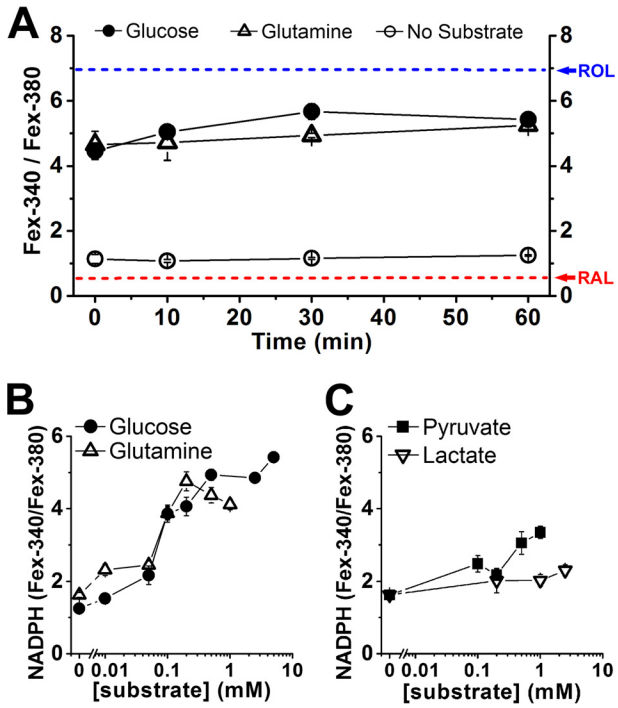

FIGURE 6. **Measurement of NADPH availability from the ratio Fex-340/Fex-380 of the fluorescence intensities excited by 340- and 380-nm light.** Fluorescence emission was collected >420 nm. *A*, dependence of the Fex-340/Fex-380 fluorescence intensity ratio on time after bleaching in the presence of 5 mM glucose (●, $n = 8$ cells), 0.2 mM glutamine (△, $n = 7$ cells), and without any substrate (○, $n = 9$ cells). The value of the ratio at 60 min after bleaching was used as a measure of NADPH availability. The *arrows* point to the values of the ratio for RAL and ROL (Fig. 2*B*). *B*, glucose (●) and glutamine (△) support NADPH generation in a concentration-dependent manner; $n \geq 6$ cells used at each substrate concentration. *C*, pyruvate (■) and lactate (▽) support NADPH generation; $n \geq 6$ cells used at each substrate concentration. The *error bars* represent standard errors. Experiments were performed at 37 °C.

fluorescence excited by 340 and 380 nm indicate that a large proportion of retinal has not been converted to retinol (Fig. 5), reflecting a requirement of extracellular metabolic substrate availability for the generation of the requisite NADPH. Glutamine, supplied at a concentration of 0.2 mM, supports the conversion of retinal to retinol to an extent similar to that of 5 mM glucose (Fig. 5), indicating that NADPH can be provided solely by mitochondria-linked pathways.

The ratio of Fex-340/Fex-380 was measured at different times after bleaching in the presence of different concentrations of various metabolic substrates. Fig. 6*A* shows that rods using either 5 mM glucose (●, $n = 8$) or 0.2 mM glutamine (△, $n = 7$) as metabolic substrate maintain the fluorescence ratio to similar levels, in the order of 4.5–5.5. These levels correspond to retinol fractions of 0.8 – 0.9 (Equation 5); that is, most of the released retinal is converted to retinol. These values of the fluorescence ratio (and retinol fraction) further correspond to an NADPH fraction of 0.1–0.2 (Equation 6). Metabolically intact rods bleached in the absence of any extracellular metabolic substrate achieved a fluorescence ratio of 1.1–1.3, corresponding to an NADPH fraction of ~0.01 (Fig. 6*A*; ○, $n = 9$). At 60 min after bleaching, the ratio in the absence of metabolic substrate had a value of 1.25 ± 0.02, significantly lower than the ratios in the presence of 5 mM glucose ($p < 0.001$) or 0.2 mM glutamine ($p < 0.001$). It was, however, significantly higher ($p < 0.001$) than the one for broken off rod outer segments (0.72 ± 0.01 at 60 min after bleaching, $n = 6$; Fig. 2*D*), indicating some ongoing metabolic activity even in the absence of any extracellular metabolic substrate.

We have used the value of the Fex-340/Fex-380 fluorescence ratio at 60 min after bleaching as a measure of NADPH availability. By that time, almost all of the retinal has been released from photoactivated rhodopsin (16). Because there is a large amount of retinal released from photoactivated rhodopsin after bleaching and a large fraction of it is present as retinol at any given time (Fig. 6*A*), the maintenance of a stable value of the NADPH fraction over time reflects continued regeneration of NADPH by the metabolic machinery of the cell. Thus, NADPH availability depends on the NADPH-generating capacity of the cell.

The availability of NADPH, as measured by the Fex-340/Fex-380 ratio, depended on the extracellular concentration of metabolic substrate. Glucose and glutamine were approximately equally effective at supporting metabolic activity, with NADPH availability being severely compromised at extracellular concentrations below ~0.1 mM (Fig. 6*B*). Pyruvate and lactate, which would both be utilized only through mitochondrial pathways, could also support some NADPH generation, but only at higher concentrations (Fig. 6*C*). Citrate and malate were much less effective at supporting NADPH generation: 2.5 mM citrate did not support significant NADPH generation, as judged by a fluorescence ratio of 0.88 ± 0.03 at 60 min after bleaching ($n = 5$), whereas 2.5 mM malate provided only modest support, as indicated by a fluorescence ratio of 1.43 ± 0.08 at 60 min after bleaching ($n = 5$) (data not shown). For experiments using glutamine, pyruvate or lactate as metabolic substrates, the solutions contained 5 mM 2-deoxyglucose, to inhibit any NADPH generation through the pentose phosphate pathway from any remaining intracellular glucose. In control experiments with selected concentrations of these substrates, omitting 2-deoxyglucose had no effect on NADPH availability, suggesting that

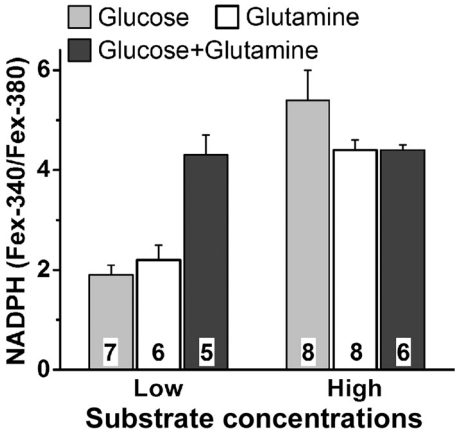

FIGURE 7. **Additive effect of glucose and glutamine on NADPH availability at low but not at high concentrations.** NADPH availability was measured from the Fex-340/Fex-380 ratio of rod outer segment fluorescence (emission, >420 nm), 60 min after bleaching. Low concentrations were 50 μM glucose and 50 μM glutamine; high concentrations were 5 mM glucose and 0.5 mM glutamine. Cell numbers are shown within each column. The *error bars* represent standard errors. Experiments were performed at 37 °C.

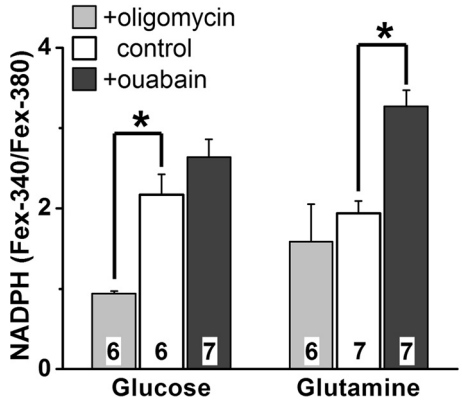

FIGURE 8. **Oligomycin suppresses and ouabain enhances NADPH generation.** NADPH generation was measured from its availability as the Fex-340/Fex-380 ratio of rod outer segment fluorescence (emission, >420 nm), 60 min after bleaching. Metabolic substrate (glucose or glutamine) concentration was 50 μM. Oligomycin and ouabain concentrations were 5 μM and 0.1 mM, respectively. Cell numbers are shown within each column. *Error bars* represent standard errors. Experiments were performed at 37 °C.

there was negligible intracellular glucose remaining (data not shown).

Although NADPH availability depends on its continuous regeneration by the metabolic machinery, factors other than metabolic activity appear to contribute to its level of availability in the rod outer segment. This is evidenced by the leveling off of the Fex-340/Fex-380 ratio at higher glucose concentrations, and interestingly, the ratio leveled off at the same values with glutamine as with glucose. Moreover, the value of the ratio did not increase when the cells were supplied with high concentrations of glucose (5 mM) and glutamine (0.5 mM) together (Fig. 7). This is somewhat surprising, because with glucose as substrate, NADPH can be generated by the pentose phosphate pathway in addition to the mitochondria-linked pathways. The experiments described below demonstrated that the pentose phosphate pathway actually makes a sizeable contribution to NADPH generation (see Fig. 9 below). Possible reasons for the leveling off are examined in more detail below (see "Discussion"). At low glucose and glutamine concentrations, it appears that metabolic substrate availability becomes limiting and NADPH availability becomes restricted by its generation, hence the drastic decline in NADPH availability below ~0.1 mM glucose or glutamine. This interpretation was reinforced by the additive effect of low (50 μM) concentrations of glucose and glutamine on NADPH availability when supplied together (Fig. 7).

Competition between ATP-generating and NADPH-generating Pathways—Because the same substrates used for the generation of NADPH are used for the generation of ATP (Fig. 1), the two processes might be expected to compete for metabolic substrate. Thus, we reasoned that inhibition of mitochondrial ATP synthesis would result in drawing off substrate to be used for ATP synthesis through glycolysis, suppressing NADPH generation. On the other hand, inhibition of ATP consumption would result in availability of substrate, augmenting NADPH generation. To experimentally resolve both decreases and increases in NADPH generation, glucose and glutamine concentrations of 50 μM were used; with this substrate concentration, the cells achieve Fex-340/Fex-380 ratios above the minimum and below the maximum values (Fig. 6*B*). Using 50 μM glucose as substrate (Fig. 8), the cells achieved a fluorescence ratio of 2.2 ± 0.3, corresponding to an NADPH fraction of 0.03. In the presence of oligomycin (5 μM), an inhibitor of the mitochondrial ATP synthase (17), the fluorescence ratio was significantly lower ($p = 0.001$), 0.94 ± 0.03, corresponding to an NADPH fraction of ~0.01. This is consistent with the inhibition of mitochondrial ATP synthesis resulting in more glucose being utilized for ATP production through glycolysis, instead of for NADPH production through the pentose phosphate pathway. For cells exposed to 0.1 mM ouabain, an inhibitor of the Na^+/K^+-ATPase (18, 19), the ratio was higher (but not significantly so, $p = 0.24$), 2.6 ± 0.2, corresponding to an NADPH fraction of 0.04. This suggests that inhibition of ATP consumption reduces the need for ATP synthesis, and glucose can be diverted for NADPH generation. Similar results were obtained with glutamine as substrate (Fig. 8), in which case both ATP and NADPH are generated by mitochondrial pathways. No 2-deoxyglucose was added in the extracellular solution in these experiments. With 50 μM glutamine as substrate, the cells achieved a fluorescence ratio of 1.9 ± 0.2, reflecting an NADPH fraction of 0.02. Inhibition of ATP synthesis with 5 μM oligomycin, resulted in a slightly lower, 1.6 ± 0.5, but not significantly different fluorescence ratio. The considerably high variability in the Fex-340/Fex-380 ratio likely reflects the strain on the cells because of inhibition of the ATP synthase, which would be the sole source of ATP with glutamine as substrate. Inhibition of ATP consumption with 0.1 mM ouabain increased the fluorescence ratio to 3.3 ± 0.2, a significantly higher value ($p < 0.001$), which reflects an NADPH fraction of 0.06.

Mitochondria Contribute to NADPH Generation Even When the Pentose Phosphate Pathway Is Operational—The experiments with glutamine (Fig. 6, *A* and *B*) demonstrate that mitochondria-linked pathways can by themselves generate quantities of NADPH comparable to those generated with glucose as primary substrate. It is not clear, however, whether the NADPH generated with glucose originates from mitochondria-linked pathways, the pentose phosphate pathway, or both. We

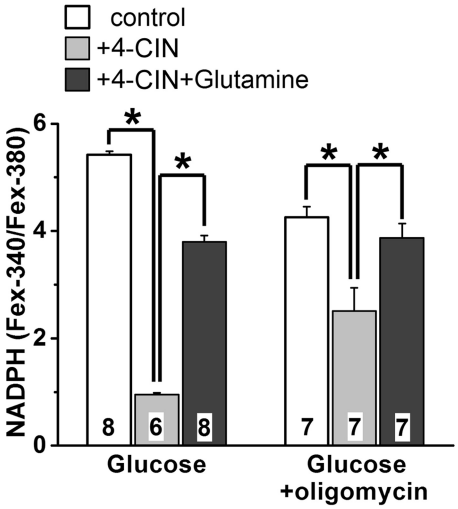

FIGURE 9. **Glutamine reverses the suppression of NADPH generation by 4-CIN.** NADPH generation was measured from its availability as the Fex-340/Fex-380 ratio of rod outer segment fluorescence (emission, >420 nm), 60 min after bleaching. Glucose and glutamine concentrations were 5.0 and 0.5 mM, respectively. Oligomycin and 4-CIN concentrations were 5 μM and 1.0 mM, respectively. Cell numbers are shown within each column. *Error bars* represent standard errors. Experiments were performed at 37 °C.

addressed this question by inhibiting the transport of pyruvate into mitochondria with 4-CIN, a monocarboxylate transporter inhibitor (20). Such a treatment would also be expected to affect ATP levels, but ATP generation by glycolysis appears to be able to compensate almost fully under conditions of mitochondrial blockage in the retina (21, 22). With 5 mM glucose as substrate and in the presence of 4-CIN, NADPH availability dropped significantly ($p < 0.001$) and resulted in a Fex-340/Fex-380 ratio of 0.95 ± 0.03, corresponding to an NADPH fraction of ~0.01 (Fig. 9). Interestingly, these levels were lower than those in the absence of any extracellular substrate, which had a fluorescence ratio of 1.25 ± 0.02 (Fig. 6*A*). A likely explanation for this result is that the lack of any metabolite entry into the mitochondria not only eliminated the mitochondrial ATP and NADPH contributions but also led to reversal of the ATP synthase. The reversed synthase drew on the ATP generated by glycolysis, finally resulting in lower availability of glucose for NADPH production. Bypassing the blocked pyruvate transporter by supplying the mitochondria directly with 0.5 mM glutamine restored the NADPH supply, as reflected in a Fex-340/Fex-380 ratio of 3.79 ± 0.12 ($p < 0.001$) and an NADPH fraction of 0.08. Restoration of the NADPH supply with glutamine under these conditions was only partial when compared with 5 mM glucose or to 0.5 mM glutamine by itself, a result that was probably due to the partial inhibition of plasma membrane monocarboxylate transporters by 4-CIN (Ref. 22; also see below).

The same experiment was carried out in the presence of oligomycin (5 μM) to inhibit the mitochondrial ATP synthase and eliminate both ATP production and ATP consumption by the enzyme. In this way, mitochondrial metabolic contributions were limited to NADPH. With 5 mM glucose as substrate and in the presence of oligomycin NADPH availability decreased, resulting in a Fex-340/Fex-380 ratio of 4.26 ± 0.19, which corresponds to an NADPH fraction of ~0.10 (Fig. 9). Inhibition of pyruvate transport resulted in a significantly lower ($p = 0.002$) Fex-340/Fex-380 ratio of 2.51 ± 0.42 (NADPH fraction of 0.03), indicating that mitochondria-linked pathways are contributing to the generation of NADPH. In addition, this ratio was significantly higher ($p = 0.002$) than the ratio of 1.25 ± 0.02 obtained in the absence of any added substrate, suggesting that the pentose phosphate pathway also contributes to the generation of NADPH. Bypassing the blocked pyruvate transporter with 0.5 mM glutamine restored the availability of NADPH, shown by a Fex-340/Fex-380 ratio of 3.87 ± 0.27 ($p = 0.012$), corresponding to an NADPH fraction of 0.08 (Fig. 9). These results demonstrate that mitochondria-linked pathways not only can supply NADPH, but do so even when the pentose phosphate pathway is operational.

In the experiments (Fig. 9) with oligomycin, as in the experiments without it, glutamine restored the NADPH supply only partially. This was probably because of partial block by 1 mM 4-CIN of the entry of glutamine into the cell. This 4-CIN concentration is more than sufficient for blocking the mitochondrial pyruvate transporter (20, 22) but only partially blocks the plasma membrane monocarboxylate transporters; the latter are effectively inhibited by much higher 4-CIN concentrations (22, 23). This possibility was supported by control experiments showing that the Fex-340/Fex-380 ratio attained by cells supplied with 0.5 mM glutamine in the presence of 1 mM 4-CIN was 3.72 ± 0.13 ($n = 5$). This value was lower than the one achieved with 0.5 mM glutamine in the absence of 4-CIN (4.37 ± 0.21, $n = 8$; Fig. 6*B*) and virtually the same as the value of the ratio restored by 0.5 mM glutamine in the experiments of Fig. 9.

DISCUSSION

We have examined the contributions of different pathways that generate NADPH in single isolated mouse rods from the reduction of all-*trans*-retinal to retinol, a reaction that uses NADPH. The measurements estimate that 0.8–0.9 of all-*trans*-retinal is converted to retinol in the outer segment of metabolically intact rods, in close agreement with biochemical measurements from extracts of whole isolated retinas (12, 16). The NADPH fraction (0.1–0.2) that corresponds to this level of conversion is equivalent to a [NADPH]/[$NADP^+$] ratio of 0.11–0.25, in good agreement with histochemical measurements (24). This [NADPH]/[$NADP^+$] ratio is achieved when metabolic substrate is not limiting and when all pathways that can generate NADPH are operational. The ratio decreases when metabolic substrates become limiting or when some pathways are inhibited.

The value of the Fex-340/Fex-380 fluorescence ratio, which reflects the extent of the conversion of all-*trans*-retinal to retinol at any given time, remained approximately stable from immediately to 60 min after bleaching. Somewhat lower values of the ratio immediately after bleaching (Fig. 6*A* for glucose and glutamine) would be consistent with a slight transient buildup of all-*trans*-retinal (16), perhaps because of a lag in NADPH availability. It should be noted that at early times after bleaching, low amounts of all-*trans*-retinal have been released, and any standing pool of NADPH makes a comparatively large contribution to the reduction to retinol. By 60 min after bleaching, almost all the considerable amount of all-*trans*-retinal has been

released (16), and the conversion of retinal to retinol depends on the generation of NADPH by the metabolic machinery.

In addition to metabolic activity, other factors appear to affect the availability of NADPH in the rod outer segment. The Fex-340/Fex-380 fluorescence ratio levels off at higher glucose concentrations, reaching similar values as with glutamine (Fig. 6*B*). Moreover, combined application of high concentrations of glucose and glutamine does not increase the ratio any further (Fig. 7). The leveling off is unlikely to reflect limitations of NADPH availability caused by diffusion through the connecting cilium (Fig. 1). The cilium does not appear to provide a significant barrier to diffusion (25), and proteins equilibrate across the cilium within 3 min (26); that is, much faster than the time scale of the measurements presented here. Although the reasons for the leveling off are not clear, factors that could possibly be playing a role include the finite size of the NADP pool, saturation of the metabolic enzymes, and perhaps cellular control of the [NADPH]/[$NADP^+$] ratio.

Sources of NADPH—NADPH can be generated in the cytosol by the pentose phosphate pathway (1, 2), as well as by $NADP^+$-dependent dehydrogenases that utilize substrates provided by the mitochondria (3, 4). It had been suggested (27) that the pentose phosphate pathway in the rod outer segment could potentially supply all the NADPH reducing equivalents necessary for the reduction of all-*trans*-retinal to retinol. More recent studies have shown that glucose enters through transporter Glut-1 into the inner segment (28), where it is phosphorylated to glucose-6-phosphate by hexokinases I and II (29). Glucose-6-phosphate can then be utilized through the pentose phosphate pathway to generate NADPH from $NADP^+$. These recent results are in tune with the observations reported here (Fig. 2, *C* and *D*) and elsewhere (10, 30) that rod outer segments separated from the rest of the cell—broken off rod outer segments—fail to reduce retinal to retinol; that is, NADPH is supplied by metabolic pathways located in the inner segment.

The present study found that with glucose as substrate, the pentose phosphate pathway makes a substantial contribution to the generation of NADPH (Fig. 9). On its own, however, the pentose phosphate pathway can attain only ~40% (0.07) of the NADPH fraction of 0.18 that is generated when metabolites are available to the mitochondria as well. The inadequacy of the pentose phosphate pathway to supply sufficient amounts of NADPH is unlikely to be due to a lack of glucose, because it was measured in the presence of 5 mM glucose, at least 10 times higher than the concentrations below which NADPH availability became compromised (Fig. 6*B*). This inadequacy reflects, therefore, the limited capacity of the pathway, and NADPH generation is supplemented by pathways that depend on mitochondrial metabolic substrates (Fig. 9). These mitochondria-linked pathways likely utilize malate and isocitrate, two intermediates of the TCA cycle, which can be transported out of the mitochondria and into the cytosol; there, they are used for the generation of NADPH by $NADP^+$-dependent dehydrogenases.

Mitochondria-linked pathways contribute to the generation of NADPH when glucose is the primary metabolic substrate and can even compensate for the pentose phosphate pathway contribution with glutamine as the primary substrate (Fig. 6, *A* and *B*). Glutamine enters the inner segment through the monocarboxylate transporter MTP1 (31) and perhaps SMCT1as well (32) and is converted to glutamate by glutaminase. Glutamate dehydrogenase converts glutamate to α-ketoglutarate, which then enters the TCA cycle. In the experiments with glucose, pyruvate, or lactate as extracellular substrates, the mitochondrial metabolic substrate would be pyruvate. It would originate intracellularly from glucose through glycolysis or from the extracellular lactate and pyruvate entering the inner segment through MTP1, with lactate being converted to pyruvate by lactate dehydrogenase.

It is possible that the contributions of different pathways to NADPH generation found in the present experiments may have been partially affected by the lack of bicarbonate in the buffer solution (33, 34). In experiments with isolated rat retinas, a lack of bicarbonate resulted in ~30% decrease in ATP content, along with a decline in the rod photoreceptor light response (34). NADPH generation, however, does not appear to be substantially affected: in experiments with isolated mouse retinas, we have found that absence of bicarbonate does not affect the reduction of all-*trans*-retinal to retinol as measured by HPLC of organic retina extracts (12).

Significance of NADPH Generation by Mitochondria-linked Pathways—Glucose appears to be a singularly important metabolic substrate for photoreceptors, because even small limitations in its availability can put photoreceptor cells at high risk (35). Removal of glucose results in photoreceptor death in isolated mouse retinas, which is prevented, at least in the short term, by the addition of mitochondrial metabolites (36). Interestingly, addition of mitochondrial metabolites does not prevent the depletion of ATP caused by the withdrawal of glucose (36). NADPH generation by mitochondria-linked pathways may therefore be an important factor for maintaining photoreceptor viability.

Apart from its involvement in the reduction of all-*trans*-retinal to retinol, NADPH is needed in large amounts in photoreceptors for the synthesis of the components required for continual outer segment renewal (37). At the same time, photoreceptors need large quantities of ATP to maintain the ionic gradients (38) required for visual transduction. In their high requirement for anabolic reactions, photoreceptors resemble tumor cells, which have been known to utilize glucose as well as glutamine to meet their metabolic needs. In glioblastoma cells, with glutamine the sole metabolic substrate, NADPH is generated by cytosolic malic enzyme using the malate derived from glutaminolysis (5). The rate of NADPH production by the malic enzyme in these cells is similar to that achieved by the pentose phosphate pathway when glucose is the sole substrate. In the retina, robust $NADP^+$-dependent malate and isocitrate dehydrogenase enzyme activities have been found that are capable of supporting NADPH generation in the absence of glucose (39).

The need for the photoreceptor cell to simultaneously meet its diverse metabolic requirements was highlighted at low substrate concentrations by the competition between ATP- and NADPH-generating pathways for metabolic substrate (Fig. 8). The ability to utilize glutamine for NADPH generation would allow a cell to better withstand periods of glucose shortage. An additional protective mechanism would be provided by catabolic reactions, as suggested by the low levels of NADPH avail-

ability that persist even in the absence of metabolic substrates (Fig. 6*A*). Support for such a mechanism is also provided by the protective role found for autophagy in isolated mouse retinas (36).

The conflicting demands for ATP and NADPH may be eased in the light, when the influx of Na^+ ions and neurotransmitter release are both reduced (38). The present experiments, having been carried out after bleaching, have exposed a potential antagonism between ATP and NADPH generation even under light conditions. One might surmise that photoreceptors would be even more vulnerable to nutrient shortages in the dark.

Effectiveness of Different Metabolic Substrates—Glutamine and glucose are two of the most abundant nutrients in plasma. Glutamine has the highest plasma concentration among amino acids (40), in the order of 0.5 mM (41). In isolated photoreceptors, glucose and glutamine were both able to support NADPH generation at very low extracellular concentrations (Fig. 6*B*), but pyruvate and lactate were ineffective (Fig. 6*C*), as were malate and citrate. Glutamine, pyruvate, and lactate have all been found to support metabolic activity in isolated rat retinas (42), albeit at much higher concentrations than the ones used with isolated photoreceptor cells in the present study. Pyruvate is the metabolite utilized by the mitochondria when glucose is the primary substrate, whereas citrate is the metabolite leaving the mitochondria and is the precursor of isocitrate and malate in the cytosol (3). The relative ineffectiveness of pyruvate, lactate, malate, and citrate is therefore somewhat surprising, especially given the effectiveness of low concentrations of both glucose and glutamine. Although it is possible that the mitochondria-linked pathways that generate NADPH are more complex than what has been assumed in this paper, another plausible explanation for the ineffectiveness of these substrates would be insufficient transport into the cell. It is not clear whether a transporter for citrate and malate, such as the neuronal Na^+-coupled citrate transporter NaC2/NaCT (43, 44), is present in photoreceptors. For lactate and pyruvate, the proposed explanation would suggest that their transport into photoreceptors by the monocarboxylate transporter is not as efficient as that of glutamine. Future measurements of transporter activity would be needed to test this explanation.

Because glucose is utilized by photoreceptors even in the presence of lactate (45), transport of extracellular pyruvate and lactate into the cell would be expected to be even smaller in the presence of glucose. Indeed, cultured retinal neuronal cells show net production of lactate (46). Lactate generated by glia has been proposed to be a metabolic substrate for neurons (47–49); for photoreceptors in the retina, the lactate would be provided by the Muller cells (50). The results in the present paper indicate that, at least for the generation of NADPH, lactate may be an unlikely extracellular metabolic substrate for photoreceptors. A far more likely metabolic substrate appears to be glutamine, which can also be generated by Muller cells (51). Consistent with such a role, glutamine transport plays a significant role *in vivo*, because intravitreal injections of 4-CIN result in a decrease in glutamine metabolites in the photoreceptors (52).

In summary, we have studied the availability of NADPH in isolated single cells using fluorescence imaging. We have demonstrated that mitochondria-linked pathways contribute substantially to NADPH generation. From their support for NADPH generation, glucose and glutamine appear to be the preferred extracellular substrates for rod photoreceptor metabolism. When extracellular metabolic substrate is limiting, there is competition between ATP- and NADPH-generating pathways. Our findings highlight the importance of mitochondria-linked pathways for the generation of NADPH in nondividing cells with a high demand for synthetic reactions. The ability to utilize substrates other than glucose is likely to play an essential role in maintaining cell functions and viability under conditions of metabolic limitations. In the retina, they could play an important role in protecting against retinal degeneration.

Acknowledgments—We thank Drs. Rosalie Crouch and Masahiro Kono for critical reading of the manuscript.

REFERENCES

1. Stanton, R. C. (2012) Glucose-6-phosphate dehydrogenase, NADPH, and cell survival. *IUBMB Life* **64,** 362–369
2. Nelson, D. L., and Cox, M. M. (2000) *Lehninger Principles of Biochemistry*, pp. 558–562, Worth, New York
3. Lunt, S. Y., and Vander Heiden, M. G. (2011) Aerobic glycolysis. Meeting the metabolic requirements of cell proliferation. *Annu. Rev. Cell Dev. Biol.* **27,** 441–464
4. Vander Heiden, M. G., Cantley, L. C., and Thompson, C. B. (2009) Understanding the Warburg effect. The metabolic requirements of cell proliferation. *Science* **324,** 1029–1033
5. DeBerardinis, R. J., Mancuso, A., Daikhin, E., Nissim, I., Yudkoff, M., Wehrli, S., and Thompson, C. B. (2007) Beyond aerobic glycolysis. Transformed cells can engage in glutamine metabolism that exceeds the requirement for protein and nucleotide synthesis. *Proc. Natl. Acad. Sci. U.S.A.* **104,** 19345–19350
6. Ebrey, T., and Koutalos, Y. (2001) Vertebrate photoreceptors. *Prog. Retin. Eye Res.* **20,** 49–94
7. Lem, J., Krasnoperova, N. V., Calvert, P. D., Kosaras, B., Cameron, D. A., Nicolò, M., Makino, C. L., and Sidman, R. L. (1999) Morphological, physiological, and biochemical changes in rhodopsin knockout mice. *Proc. Natl. Acad. Sci. U.S.A.* **96,** 736–741
8. Futterman, S., Hendrickson, A., Bishop, P. E., Rollins, M. H., and Vacano, E. (1970) Metabolism of glucose and reduction of retinaldehyde in retinal photoreceptors. *J. Neurochem.* **17,** 149–156
9. Hubbard, R., Brown, P. K., and Bownds, D. (1971) Methodology of vitamin A and visual pigments. *Methods Enzymol.* **18C,** 615–653
10. Chen, C., and Koutalos, Y. (2010) Rapid formation of all-trans retinol after bleaching in frog and mouse rod photoreceptor outer segments. *Photochem. Photobiol. Sci.* **9,** 1475–1479
11. Chen, C., Thompson, D. A., and Koutalos, Y. (2012) Reduction of all-*trans*-retinal in vertebrate rod photoreceptors requires the combined action of RDH8 and RDH12. *J. Biol. Chem.* **287,** 24662–24670
12. Chen, C., Blakeley, L. R., and Koutalos, Y. (2009) Formation of all-*trans* retinol after visual pigment bleaching in mouse photoreceptors. *Invest. Ophthalmol. Vis. Sci.* **50,** 3589–3595
13. Chen, C., Jiang, Y., and Koutalos, Y. (2002) Dynamic behavior of rod photoreceptor disks. *Biophys. J.* **83,** 1403–1412
14. Redmond, T. M., Yu, S., Lee, E., Bok, D., Hamasaki, D., Chen, N., Goletz, P., Ma, J. X., Crouch, R. K., and Pfeifer, K. (1998) Rpe65 is necessary for production of 11-*cis*-vitamin A in the retinal visual cycle. *Nat. Genet.* **20,** 344–351
15. Bliss, A. F. (1951) The equilibrium between vitamin A alcohol and aldehyde in the presence of alcohol dehydrogenase. *Arch. Biochem.* **31,** 197–204
16. Blakeley, L. R., Chen, C., Chen, C. K., Chen, J., Crouch, R. K., Travis, G. H., and Koutalos, Y. (2011) Rod outer segment retinol formation is independent of Abca4, arrestin, rhodopsin kinase, and rhodopsin palmitylation.

Invest. Ophthalmol. Vis. Sci. **52,** 3483–3491
17. Kagawa, Y., and Racker, E. (1966) Partial resolution of the enzymes catalyzing oxidative phosphorylation. 8. Properties of a factor conferring oligomycin sensitivity on mitochondrial adenosine triphosphatase. *J. Biol. Chem.* **241,** 2461–2466
18. Demontis, G. C., Ratto, G. M., Bisti, S., and Cervetto, L. (1995) Effect of blocking the Na^+/K^+ ATPase on Ca^{2+} extrusion and light adaptation in mammalian retinal rods. *Biophys. J.* **69,** 439–450
19. Winkler, B. S. (1983) Relative inhibitory effects of ATP depletion, ouabain and calcium on retinal photoreceptors. *Exp. Eye Res.* **36,** 581–594
20. Halestrap, A. P., and Denton, R. M. (1975) The specificity and metabolic implications of the inhibition of pyruvate transport in isolated mitochondria and intact tissue preparations by alpha-Cyano-4-hydroxycinnamate and related compounds. *Biochem. J.* **148,** 97–106
21. Winkler, B. S., Dang, L., Malinoski, C., and Easter, S. S., Jr. (1997) An assessment of rat photoreceptor sensitivity to mitochondrial blockade. *Invest. Ophthalmol. Vis. Sci.* **38,** 1569–1577
22. Zeevalk, G. D., and Nicklas, W. J. (2000) Lactate prevents the alterations in tissue amino acids, decline in ATP, and cell damage due to aglycemia in retina. *J. Neurochem.* **75,** 1027–1034
23. Bui, B. V., Kalloniatis, M., and Vingrys, A. J. (2004) Retinal function loss after monocarboxylate transport inhibition. *Invest. Ophthalmol. Vis. Sci.* **45,** 584–593
24. Matschinsky, F. M. (1968) Quantitative histochemistry of nicotinamide adenine nucleotides in retina of monkey and rabbit. *J. Neurochem.* **15,** 643–657
25. Calvert, P. D., Schiesser, W. E., and Pugh, E. N., Jr. (2010) Diffusion of a soluble protein, photoactivatable GFP, through a sensory cilium. *J. Gen. Physiol.* **135,** 173–196
26. Nair, K. S., Hanson, S. M., Mendez, A., Gurevich, E. V., Kennedy, M. J., Shestopalov, V. I., Vishnivetskiy, S. A., Chen, J., Hurley, J. B., Gurevich, V. V., and Slepak, V. Z. (2005) Light-dependent redistribution of arrestin in vertebrate rods is an energy-independent process governed by protein-protein interactions. *Neuron* **46,** 555–567
27. Hsu, S. C., and Molday, R. S. (1994) Glucose metabolism in photoreceptor outer segments. Its role in phototransduction and in NADPH-requiring reactions. *J. Biol. Chem.* **269,** 17954–17959
28. Gospe, S. M., 3rd, Baker, S. A., and Arshavsky, V. Y. (2010) Facilitative glucose transporter Glut1 is actively excluded from rod outer segments. *J. Cell Sci.* **123,** 3639–3644
29. Reidel, B., Thompson, J. W., Farsiu, S., Moseley, M. A., Skiba, N. P., and Arshavsky, V. Y. (2011) Proteomic profiling of a layered tissue reveals unique glycolytic specializations of photoreceptor cells. *Mol. Cell. Proteomics* 10.1074/mcp.M110.002469
30. Tsina, E., Chen, C., Koutalos, Y., Ala-Laurila, P., Tsacopoulos, M., Wiggert, B., Crouch, R. K., and Cornwall, M. C. (2004) Physiological and microfluorometric studies of reduction and clearance of retinal in bleached rod photoreceptors. *J. Gen. Physiol.* **124,** 429–443
31. Bergersen, L., Jóhannsson, E., Veruki, M. L., Nagelhus, E. A., Halestrap, A., Sejersted, O. M., and Ottersen, O. P. (1999) Cellular and subcellular expression of monocarboxylate transporters in the pigment epithelium and retina of the rat. *Neuroscience* **90,** 319–331
32. Martin, P. M., Dun, Y., Mysona, B., Ananth, S., Roon, P., Smith, S. B., and Ganapathy, V. (2007) Expression of the sodium-coupled monocarboxylate transporters SMCT1 (SLC5A8) and SMCT2 (SLC5A12) in retina. *Invest. Ophthalmol. Vis. Sci.* **48,** 3356–3363
33. Winkler, B. S. (1986) Buffer dependence of retinal glycolysis and ERG potentials. *Exp. Eye Res.* **42,** 585–593
34. Winkler, B. S., Simson, V., and Benner, J. (1977) Importance of bicarbonate in retinal function. *Invest. Ophthalmol. Vis. Sci.* **16,** 766–768
35. Winkler, B. S., Sauer, M. W., and Starnes, C. A. (2003) Modulation of the Pasteur effect in retinal cells. Implications for understanding compensatory metabolic mechanisms. *Exp. Eye Res.* **76,** 715–723
36. Chertov, A. O., Holzhausen, L., Kuok, I. T., Couron, D., Parker, E., Linton, J. D., Sadilek, M., Sweet, I. R., and Hurley, J. B. (2011) Roles of glucose in photoreceptor survival. *J. Biol. Chem.* **286,** 34700–34711
37. Young, R. W. (1967) The renewal of photoreceptor cell outer segments. *J. Cell Biol.* **33,** 61–72
38. Okawa, H., Sampath, A. P., Laughlin, S. B., and Fain, G. L. (2008) ATP consumption by mammalian rod photoreceptors in darkness and in light. *Curr. Biol.* **18,** 1917–1921
39. Winkler, B. S., DeSantis, N., and Solomon, F. (1986) Multiple NADPH-producing pathways control glutathione (GSH) content in retina. *Exp. Eye Res.* **43,** 829–847
40. Stein, W. H., and Moore, S. (1954) The free amino acids of human blood plasma. *J. Biol. Chem.* **211,** 915–926
41. Archibald, R. M. (1944) The enzymatic determination of glutamine. *J. Biol. Chem.* **154,** 643–656
42. Winkler, B. S. (1981) Glycolytic and oxidative metabolism in relation to retinal function. *J. Gen. Physiol.* **77,** 667–692
43. Inoue, K., Zhuang, L., Maddox, D. M., Smith, S. B., and Ganapathy, V. (2002) Structure, function, and expression pattern of a novel sodium-coupled citrate transporter (NaCT) cloned from mammalian brain. *J. Biol. Chem.* **277,** 39469–39476
44. Wada, M., Shimada, A., and Fujita, T. (2006) Functional characterization of Na^+-coupled citrate transporter NaC2/NaCT expressed in primary cultures of neurons from mouse cerebral cortex. *Brain Res.* **1081,** 92–100
45. Winkler, B. S., Pourcho, R. G., Starnes, C., Slocum, J., and Slocum, N. (2003) Metabolic mapping in mammalian retina. A biochemical and ^{3}H-2-deoxyglucose autoradiographic study. *Exp. Eye Res.* **77,** 327–337
46. Winkler, B. S., Starnes, C. A., Sauer, M. W., Firouzgan, Z., and Chen, S. C. (2004) Cultured retinal neuronal cells and Muller cells both show net production of lactate. *Neurochem. Int.* **45,** 311–320
47. Schurr, A., Miller, J. J., Payne, R. S., and Rigor, B. M. (1999) An increase in lactate output by brain tissue serves to meet the energy needs of glutamate-activated neurons. *J. Neurosci.* **19,** 34–39
48. Tsacopoulos, M., and Magistretti, P. J. (1996) Metabolic coupling between glia and neurons. *J. Neurosci.* **16,** 877–885
49. Wyss, M. T., Jolivet, R., Buck, A., Magistretti, P. J., and Weber, B. (2011) *In vivo* evidence for lactate as a neuronal energy source. *J. Neurosci.* **31,** 7477–7485
50. Poitry-Yamate, C. L., Poitry, S., and Tsacopoulos, M. (1995) Lactate released by Muller glial cells is metabolized by photoreceptors from mammalian retina. *J. Neurosci.* **15,** 5179–5191
51. Poitry, S., Poitry-Yamate, C., Ueberfeld, J., MacLeish, P. R., and Tsacopoulos, M. (2000) Mechanisms of glutamate metabolic signaling in retinal glial (Muller) cells. *J. Neurosci.* **20,** 1809–1821
52. Bui, B. V., Vingrys, A. J., Wellard, J. W., and Kalloniatis, M. (2004) Monocarboxylate transport inhibition alters retinal function and cellular amino acid levels. *Eur. J. Neurosci.* **20,** 1525–1537